

<https://doi.org/10.48047/Afjbs.6.Si4.2024.6656-6662>



## African Journal of Biological Sciences



# Studies on Growth, Spectral and Optical Studies of Propyl Triphenylphosphonium Bromide Single Crystals for Nonlinear Optical Applications

G. Santhana Krishnan <sup>1</sup>, S. Hemavathy <sup>1</sup>, M. Mohanraj <sup>2</sup>, M. Parthasarathy <sup>3\*</sup>

<sup>1,2,3\*</sup>Department of Physics, School of Basic Sciences, Vels Institute of Science, Technology and Advanced Studies (VISTAS), Pallavaram, Chennai – 600 117, Tamilnadu, India.

\*Corresponding Author: Dr M Parthasarathy

\*Email: mps2k7@gmail.com

#### Article History

Volume 6, Issue 4s, September 2024

Received: 15 July 2024

Accepted: 25 Aug 2024

Published: 25 Sep 2024

doi:10.48047/Afjbs.6.Si4.2024.6656-6662

#### ABSTRACT

A good quality single crystal of Propyl triphenylphosphonium bromide (PTPB) was grown using a low-temperature solution technique with an aqueous solution at room temperature. The as-grown single crystal belongs to the monoclinic system with space group P21/c, as confirmed by single crystal X-ray diffraction. FT-IR spectral analysis confirmed the presence of various functional groups in the grown crystal. Additionally, optical characteristics were evaluated using UV-visible analysis. The lower cut-off wavelength observed in the spectrum was 312 nm, with an optical bandgap of 4 eV. The Urbach energy of the grown crystal was found to be minimal, indicating good crystallinity. Furthermore, the electron-phonon interaction energy was also estimated.

Keywords: Single crystal growth, FT-IR, Band gap energy, Urbach energy, Refractive index

## 1. INTRODUCTION

The fields of optoelectronics, telecommunications, and the laser industry have significantly benefited from the utilization of nonlinear optical materials [1–3]. In recent years, the search for NLO materials with substantial second- and third-order optical nonlinearities and rapid response times has become crucial for technological advancements. The unique combination of enhanced properties from both organic and inorganic crystals in semi-organic materials, such as high damage threshold, wide transparency range, lower UV cutoff wavelength, high nonlinear coefficient, high mechanical stability, and high thermal stability, make them highly suitable for frequency doubling and device fabrication.

Phosphonium salts are widely used as catalysts for phase transfer reactions and have applications as biocides, plant growth regulators, and in the curing of epoxy resins. The organic molecular crystals of phosphate show significant potential for various photoinduced effects due to the substantial anisotropy in the chemical bonds within the phosphate groups and the weaker

intermolecular chemical bonds. Organic ligands in semi-organic materials form hydrogen bonds with the inorganic network, leading to the development of new high-optical nonlinear materials. Amino acids are composed of zwitterions, carboxyl proton donor (COO<sup>-</sup>) and acceptor (NH<sub>2</sub>) groups, and their dipolar nature makes them suitable for nonlinear optical applications that leverage their unique physical and chemical properties [4]. The molecular structure of PTPB is shown in Figure 1.

The study conducted involved the growth of a single crystal of PTPB using the low-temperature solution method (SEST) with water as the solvent at room temperature. Subsequently, the grown crystals underwent characterization through single crystal X-ray diffraction, Fourier transform infrared (FT-IR) spectroscopic analysis, and optical assessment encompassing transmittance, absorbance, optical bandgap, Urbach energy, and refractive index for the titled crystal.

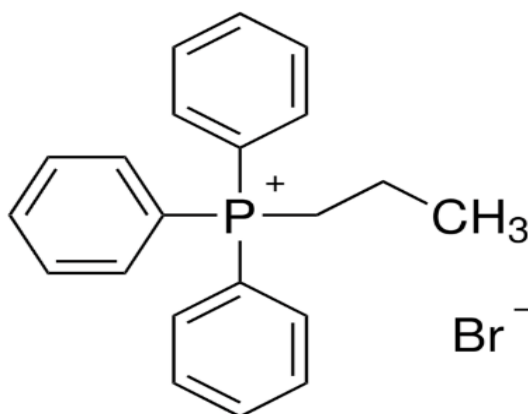


Figure 1 Molecular structure of PTPB

## 2. EXPERIMENTAL METHODS

The commercially available Propyl triphenylphosphonium bromide (Sigma Aldrich 98%) was purchased and grown as a single crystal by slow evaporation solution growth technique using water as solvent at ambient temperature. A homogeneous solution was prepared at room temperature using aqueous solution as the solvent, and the mixture was stirred using a magnetic stirrer for 8 hours. The solute's equilibrium concentration was determined using gravimetric analysis after saturation had been reached. Additionally, repeated recrystallization was performed to enhance the optical quality of the crystals. The homogeneous solution was then carefully filtered using Whatman filter paper and housed in a beaker and placed in a constant temperature bath ( $\pm 0.01^\circ\text{C}$ ). After 35 days, a good quality single crystal of Propyl triphenylphosphonium bromide was obtained from the mother solution, as illustrated in Figure 2.



Figure 2 As grown single crystal of PTPB

### 3. CHARACTERIZATION TECHNIQUES

The single crystal X-ray diffraction data of PTPB was obtained using a Bruker AXS Kappa Apex II CCD Diffractometer with MoK $\alpha$  radiation ( $\lambda = 0.7107 \text{ \AA}$ ) as the monochromatic source. The FT-IR spectrum was analysed within the range of 400 – 4000  $\text{cm}^{-1}$ , and the UV-Visible spectra were examined using the Perkin Elmer LAMBDA 950 Spectrophotometer across the wavelength range of 200 nm to 800 nm.

### 4. RESULTS AND DISCUSSION

#### 4.1 Single crystal X-ray diffraction analysis

The as grown single crystal of PTPB was subjected to x-ray diffraction using Bruker Kappa APEX II diffractometer. From the studies, it crystallizes in the monoclinic system with space group  $P2_1/c$ . The calculated cell parameters  $a = 10.87 \text{ \AA}$ ,  $b = 10.00 \text{ \AA}$ ,  $c = 18.01 \text{ \AA}$ ,  $\alpha = \beta = 90^\circ$ ,  $\gamma = 104^\circ$  and  $V = 1898 \text{ \AA}^3$  are well matched with the reported literature values [6], which is tabulated in Table 1.

Table 1 Crystallographic information of PTPB

Lattice parameters	Present work	Edmund W. Czerwinski (2004)
a	10.87 $\text{\AA}$	10.79 $\text{\AA}$
b	10.00 $\text{\AA}$	9.85 $\text{\AA}$
c	18.01 $\text{\AA}$	17.86 $\text{\AA}$
Crystal system with space group	Monoclinic, $P2_1/c$	Monoclinic, $P2_1/c$
$\alpha = \beta$	$90^\circ$	$90^\circ$
$\gamma$	$104^\circ$	$103.96^\circ$
Volume	$1898 \text{ \AA}^3$	$1844 \text{ \AA}^3$

#### 4.2 FT-IR spectral analysis

The FT-IR spectrum of the title compound (PTPB) was recorded in the range of 400 to 4000  $\text{cm}^{-1}$  using a Bruker AXS FT-IR spectrophotometer, as shown in Figure 3. The asymmetric stretching vibrations of  $\text{NH}_2$  typically occur in the range of 3099–3051  $\text{cm}^{-1}$ , while the symmetric stretching vibrations of  $\text{NH}_2$  are observed around 3051  $\text{cm}^{-1}$ . The position, broadness, and wavenumber of this vibration indicate the formation of a strong intramolecular N-H-Cl hydrogen bonding between the  $\text{NH}_3^+$  group and the  $\text{Br}^-$ . The lower wavenumber of this mode suggests the presence of a strong hydrogen bonding geometry. The strong intermolecular and intramolecular N-H-Br hydrogen bonding contributes to the non-centrosymmetric structure of PTPB and enhances its molecular hyperpolarizability [7, 8]. A faint band at 1587  $\text{cm}^{-1}$  corresponds to the asymmetric bending mode of the  $\text{NH}_3^+$  ion, while the relatively intense band observed at 1148  $\text{cm}^{-1}$  is assigned to the symmetric bending mode of  $\text{NH}_3^+$ . The wavenumber range of 1146–1109  $\text{cm}^{-1}$  encompasses the rocking vibrational modes of  $\text{NH}_3^+$  [9–11].

The formation of the quaternary phosphonium groups,  $\text{P}^+ \text{PH}_3 \text{Br}^-$ , as confirmed by the appearance of the absorption peaks at 1430  $\text{cm}^{-1}$  and 1109  $\text{cm}^{-1}$ . Vibrational tension of the C-H and C-C links are confirmed by the peaks at 3051  $\text{cm}^{-1}$  and 1587  $\text{cm}^{-1}$  respectively. The vibrational tension of the  $-\text{C} = \text{C}$  conjugated double bond is confirmed by the peak at 1481  $\text{cm}^{-1}$ . Peaks at 844  $\text{cm}^{-1}$  (strong) and 1146  $\text{cm}^{-1}$  – 1109  $\text{cm}^{-1}$  (weak), and the strong band at 691  $\text{cm}^{-1}$  correspond to the vibration in plane and out of the plane, respectively, of the C-H bonds.

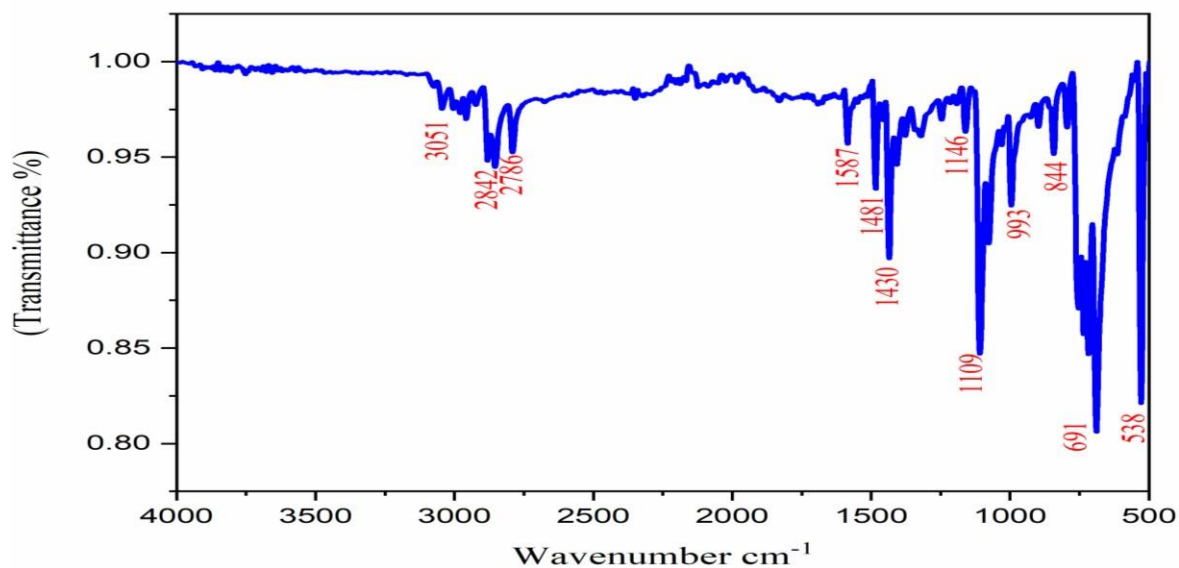


Figure 3 FT-IR spectrum of PTPB

#### 4.3 Optical absorption spectra

The optical studies were conducted using a Perkin-Elmer Lambda-35 UV-Visible spectrophotometer in the wavelength range of 200 – 800 nm. The UV-visible spectrum provides information about the molecule's structure because the absorption of UV and visible light involves the promotion of the electron from the ground state to higher states. Figure 4 shows the UV-Visible absorbance spectrum of PTPB. From the spectrum, the cut off wavelength was observed at 312 nm. From the transmittance spectrum (Figure 5), The grown crystal exhibited good transmittance throughout the entire visible region for NLO, optoelectronic, and other applications [12-15].

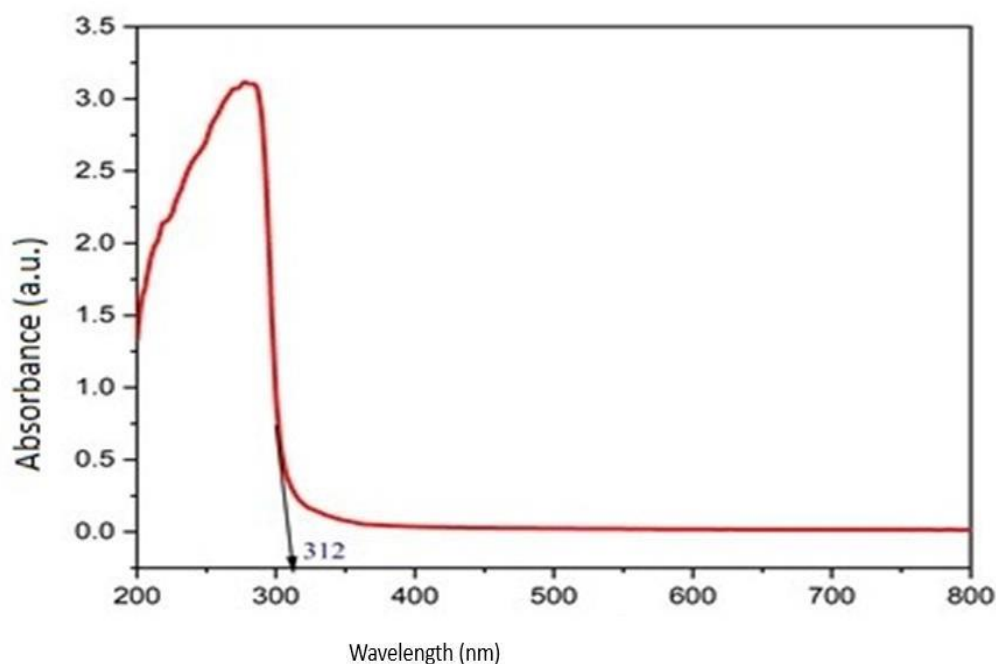


Figure 4 UV-Visible absorbance spectrum of PTPB

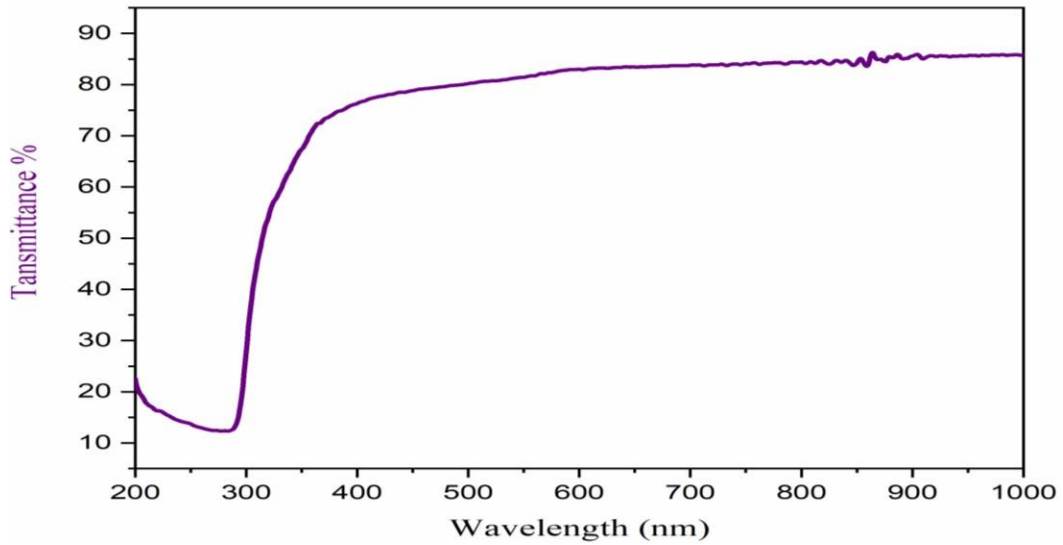


Figure 5 UV-Visible transmittance spectrum of PTPB

The UV-visible absorbance data was used to calculate the optical band gap, which is shown in Figure 6. The plot of energy ( $h\nu$ ) versus  $(\alpha h\nu)^{1/2}$ , where " $\alpha$ " represents the absorption coefficient, helped determine the optical band gap energy, which was found to be 4 eV by extrapolating the slope region where it intersects the x-axis. In Figure 7, the relationship between refractive index ( $n$ ) and wavelength ( $\lambda$ ) is depicted. The spectrum shows the refractive index ( $n$ ) as a function of wavelength ( $\lambda$ ).

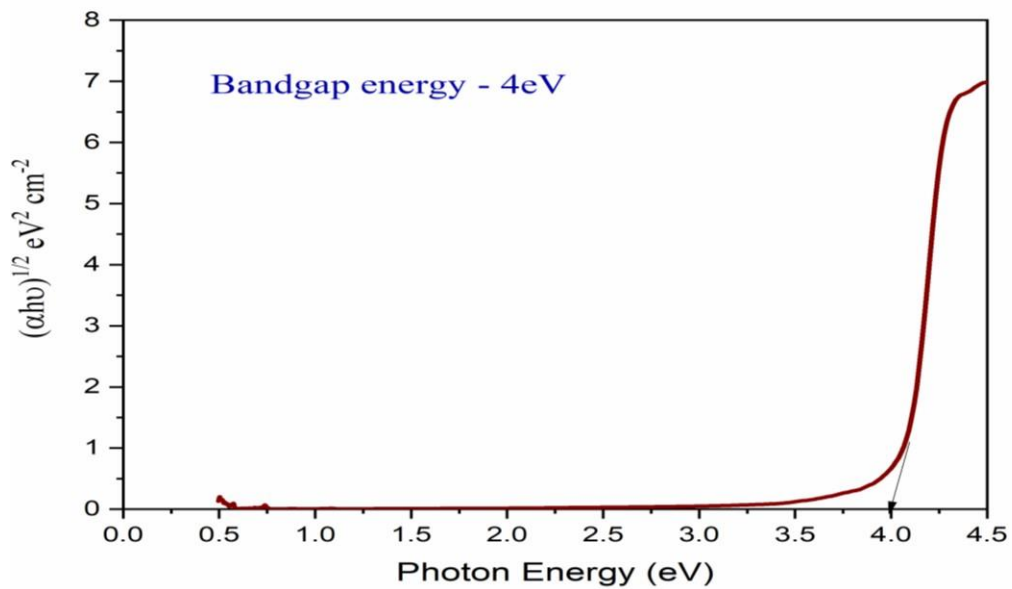


Figure 6. Variation of Photon energy ( $h\nu$ ) with  $(\alpha h\nu)^{1/2}$

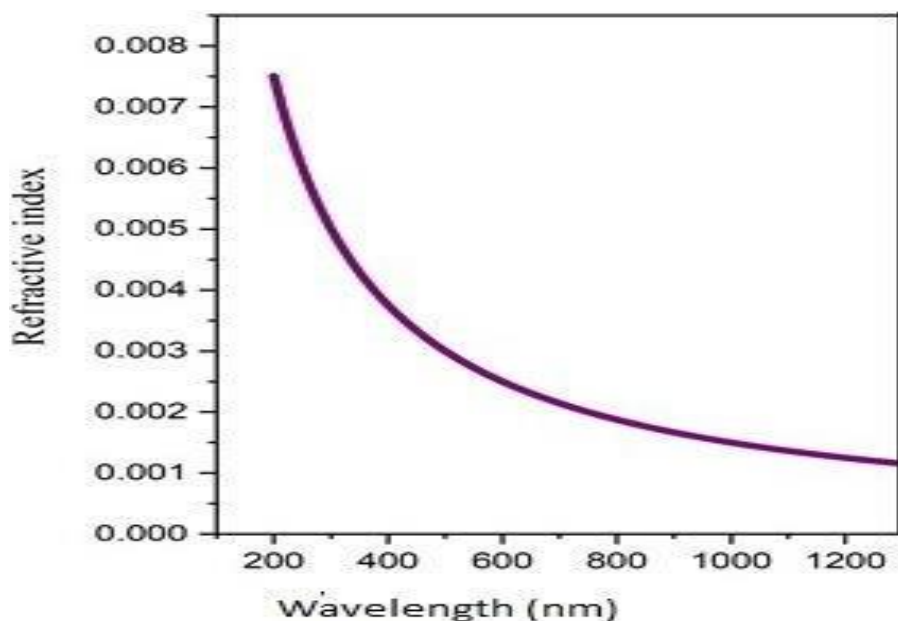


Figure 7. Wavelength dependence of PTPB

#### 4.4 Absorption band tail (Urbach energy)

Optical absorption plays a crucial role in material science as it determines a material's suitability for optical applications by providing essential information about the optical band gap. The optical absorption spectra of materials can be categorized into three main regions. The weak absorption region is caused by defects and impurities within the materials. The absorption edge region arises due to perturbations in the structure and disorder of the system. Finally, the strong absorption region helps determine the energy of the optical band gap.

The absorption coefficient curve near the optical band edge exhibits an exponential feature known as the Urbach tail. This tail is more pronounced in poorly crystalline and amorphous materials, indicating a higher degree of lattice disorder. Conversely, a minimal Urbach tail suggests good crystalline quality and lattice perfection [16–17]. The relationship between  $\alpha$  and the energy of photons ( $h\nu$ ) near the optical band gap edge is described by the Urbach empirical rule. The Urbach energy (EU), representing the band tail energy, is determined by taking the reciprocal of the slope of the  $\ln(\alpha)$  versus incident photon energy ( $h\nu$ ). In this case, the value obtained was 0.164 eV as shown in Figure 8.

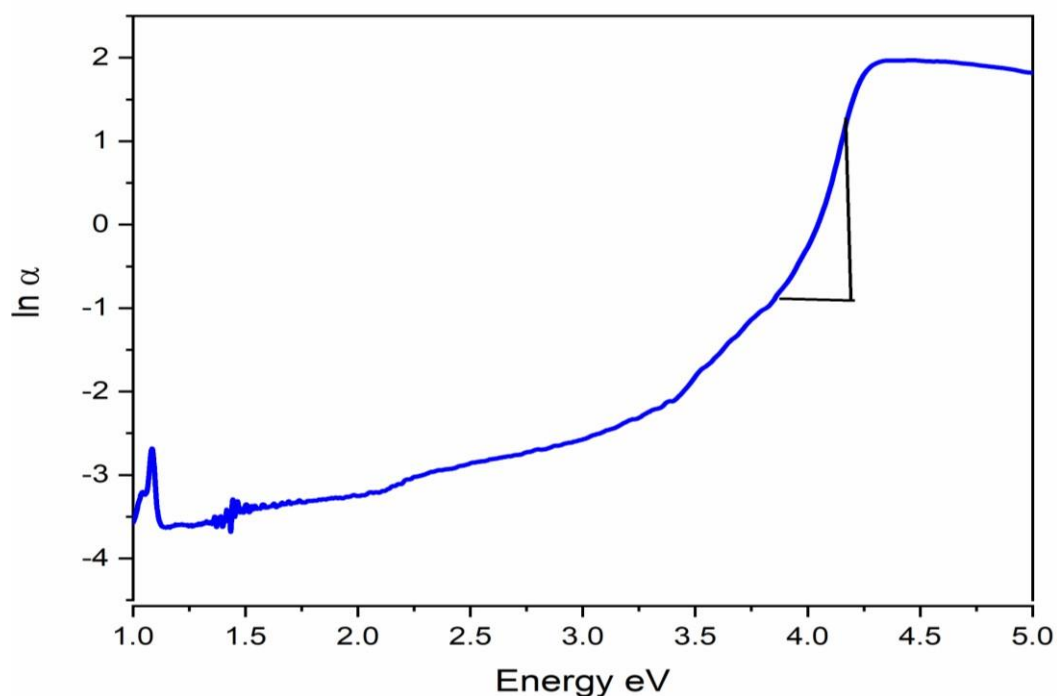


Figure 8 Urbach energy of PTPB

## 5. CONCLUSION

Good quality optical single crystal of PTPB was grown by slow evaporation solution technique at ambient temperature. Single crystal X-ray diffraction study reveals that the grown crystal belongs to Monoclinic system with space group P21/c. Functional groups were identified by using FT-IR spectral analysis. UV-Vis studies were carried out and the lower cut-off wavelength was observed at 312 nm and the optical bandgap was found to be 4 eV. The minimum of Urbach energy indicates that the grown crystal has good crystalline perfection.

## Acknowledgements

The authors are acknowledged to SAIF, IIT-Madras, Chennai – 600 036 for the data collection of single crystal X-ray diffraction. The authors extend their acknowledgment to Department of Physics, B.S. Abdur Rahman Crescent Institute of Science & Technology, Chennai – 600 048 for data collection of FT-IR and UV-Visible studies.

## REFERENCES

1. H.O. Marcy, L.F. Warren, M.S. Webb, C.A. Ebbers, S.P. Velsko, G.C. Kennedy and G.C. Catella, *Appl. Opt.* 31, 5051 (1992)
2. R.L. Sutherland, *Handbook of Nonlinear Optics*, 2nd edn. (Dekker, New York, 1996)
3. M. Krishnakumar, S. Karthick, K. Thirupugalmani, B. Babu and G. Vinitha, *Opt. Laser Technol.* 101, 91-106 (2018)
4. B.A. Fuchs, K. Chaisyn and P. Stephan Velsko, *Appl. Opt.* 28, 4465-4472 (1989)
5. D.L. Bryce, G.D. Sward and S. Adiga, *J. Am. Chem. Soc.* 128, 2121-2134 (2006)
6. Edmund W. Czerwinski, *Acta Cryst E60*, 1442-1443 . (2004).
7. D.L. Vein, N.B. Colthup, W.G. Fateley and J.G. Grasselli, *The Handbook of Infrared and Raman Characteristic Frequencies of Organic Molecules* (Academic Press, New York, 1991)
8. H. Ratajczak, J. Baran, J. Barycki, S. Debrus, M. May, A. Pietraszko, H.M. Ratajczak, A. Tramer and J. Venturini, *J. Mol. Struct.* 555, 149 (2000)

9. S. Debrus, H. Ratajczak, J. Venturini, N. Pincon, J. Baran, J. Barycki, T. Glowiak and A. Pieraszko, *Synth. Met.* 127, 99 (2002)
10. M. Tsuboi et al., *Spectrosc. Acta* 19, 271 (1963)
11. E. Steger et al., *Spectrosc. Acta* 19, 293 (1963)
12. G. Socrates, *Infrared and Raman Characteristic Group Frequencies* (Wiley, West London, 2001)
13. S.R. Yousefi, A. Sobhani, H.A. Alshamsi and M. Salavati-Niasari, *RSC Adv.* 11, 11500–11512 (2021)
14. S.R. Yousefi, M. Masjedi-Arani, M.S. Morassaei, M. Salavati-Niasari and H. Moayedi, *Int. J. Hydrog. Energy* 44, 43 (2019)
15. S.R. Yousefi, A. Sobhani and M. Salavati-Niasari, *Adv. Powder Technol.* 28(4), 1258–1262 (2017)
16. F. Urbach, *Phys. Rev.* 92 1324 (1953).
17. S.J. Ikhmayies and R.N. Ahmad-Bitar, *J. Mater. Res. Technol* 2 221–227 (2013).